Regional Studies in Marine Science 62 (2023) 102922

Contents lists available at ScienceDirect

Regional Studies in Marine Science

journal homepage: www.elsevier.com/locate/rsma

Contributions from the main river of the largest open sea delta in the Americas to the CO_2 fluxes

R.S.A. Chielle [a,*], R.V. Marins [a], F.J.S. Dias [b], K.K. Borges [b], C.E. Rezende [c]

[a] Laboratório de Biogeoquímica Costeira, Instituto de Ciências do Mar, Universidade Federal do Ceará, Avenida Abolição 3207, 60165-081, Fortaleza, Ceará, Brazil
[b] Laboratório de Hidrodinâmica Costeira, Estuarina e de Águas Interiores (LHiCEAI), Universidade Federal do Maranhão, Avenida dos Portugueses 1966, 65080-805, São Luis, Maranhão, Brazil
[c] Laboratório de Ciências Ambientais, Centro de Biociências e Biotecnologia, Universidade Estadual do Norte Fluminense Darcy Ribeiro, Av. Alberto Lamego, 2000, 28013-602 Campos dos Goytacazes RJ, Brazil

ARTICLE INFO

Article history:
Received 7 November 2022
Received in revised form 25 January 2023
Accepted 3 March 2023
Available online 6 March 2023

Keywords:
Estuary
pCO_2
Interface
Water–atmosphere
Parnaíba river
Rainy season

ABSTRACT

In this study, we sampled for the first time the main channel of the Parnaíba Delta, the largest open sea delta in the Americas, and two of its secondary channels, during the rainy season. Continuous measurements of pCO_2, temperature, salinity, and wind velocity were taken, while subsurface water samples were collected to analyze for dissolved oxygen, pH, total alkalinity, dissolved organic carbon, and its isotopic, chlorophyll-*a*, and nutrients. The spatial variability of pCO_2 along the different channels showed the existence of distinct drivers of CO_2 dynamics in the area. The correlation of pCO_2 in freshwater samples with dissolved oxygen and chlorophyll-*a* indicated the incidence of organic matter decomposition and primary production in the main channel and mangroves, while the highest salinity samples evidenced the control of carbonate equilibrium in the river mouth. Our data also indicated an important influence of the river discharge on the carbon dynamics of the estuary, with around 73% of the CO_2 emissions in the estuary estimated to be from riverine CO_2. The strong river effect in the estuary was also supported by the low salinities (0.04–26.37), pH (7.09 $\pm$ 0.36), and total alkalinity (328 $\pm$ 530.46 μmol kg^{-1}), typical from fluvial waters. The estuary was supersaturated in CO_2 and behaved as a strong source, with an average flux of 194.1 $\pm$ 135.1 mmol m^{-2} d^{-1}.

1. Introduction

Estuaries are dynamic transitional environments connecting terrestrial, riverine, oceanic, and atmospheric biogeochemical carbon cycles. They receive a large amount of terrigenous material that is transformed and exchanged with the open sea (Gattuso et al., 1998). The net heterotrophy of these environments, together with the input of CO_2-enriched freshwaters are the main reasons these systems are usually supersaturated in CO_2 (Borges and Abril, 2011; Gattuso et al., 1998). However, the global air–water CO_2 fluxes and regulating processes are still uncertain in these environments, and therefore, they have been often neglected in the global carbon budgets (Le Quéré et al., 2018).

One of the main difficulties in integrating the CO_2 fluxes in estuaries is that they have a large heterogeneity between systems, but also intrinsic variability. The spatial variability of pCO_2 in estuaries is a result of the strong gradient of biogeochemical parameters during the mix of river and seawater, being enhanced by temporal variability as the climate is one of the main drivers of CO_2 dynamics in estuaries, controlling riverine carbon supply (Bauer et al., 2013). In fact, the importance of climate to the estuarine CO_2 cycle has been reported in various studies, showing that estuaries are stronger sources of CO_2 to the atmosphere during the high discharge season than during the dry season (Borges et al., 2018; Sarma et al., 2012; Sawakuchi et al., 2017). Besides, on the equatorial Brazilian coast, even in the dry season, Carvalho et al. (2017) showed a distinct behavior of CO_2 in the continental shelf related to the transition between semi-arid and humid climate from the northeastern to the Amazonian continental shelf.

The first global estimate showed estuaries to respond for around 0.6 Pg C yr^{-1} emitted to the atmosphere (Abril and Borges, 2004). However, most recent estimates suggest these coastal environments with emissions equivalent to the sink of CO_2 taking place in continental shelves, of around 0.1 Pg C yr^{-1} (Chen et al., 2013; Laruelle et al., 2014). The great variability of estuarine emission estimates proves the need for more studies in these regions. The scarcity of data is the main limitation for a good spatial and temporal quantification of estuarine CO_2 fluxes

* Corresponding author.
E-mail address: oc.raisasiqueira@gmail.com (R.S.A. Chielle).

https://doi.org/10.1016/j.rsma.2023.102922
2352-4855/

and many large tropical estuarine systems remain unmapped regarding CO_2 dynamics, especially in the southern hemisphere. In fact, of the 163 environments considered in the most recent global estuarine emission survey (Chen et al., 2013) only 13 were in the Southern Hemisphere, and just two were from Brazilian estuaries.

In Brazil, studies regarding CO_2 in estuaries are still scarce and most of them are estimates based on the carbonate system, such as those included in global estimates (Ovalle et al., 1990; Souza et al., 2009). A few recent studies have focused on impacted environments such as Guanabara Bay (Cotovicz et al., 2015; Marotta et al., 2020) and in Southeastern Brazil, semi-arid estuaries (Cotovicz et al., 2022). Also, a few studies focused on the aquatic Amazonian systems, including freshwaters (Sawakuchi et al., 2017) and mangrove creeks (Call et al., 2019).

The Parnaíba river is the third largest river in Brazil and its delta is the largest open sea delta in the Americas. An Environmental Protection Area with 313,809 ha is inserted in the delta which preserves over 100,000 ha of mangroves and sustains great biodiversity. A recent study by Grazielle et al. (2020) showed the great potential of carbon storage by the extensive and dense mangrove vegetation in this protected area, and that the condition of a conservation area promotes this great carbon storage (258.34 Mg C ha^{-1}). Recent studies also pointed out the great influence of the river discharge on the coastal dynamics and shoreline changes (Aquino da Silva et al., 2019; da Silva et al., 2015; Ferreira et al., 2021), as well as in the quality state of the estuarine waters (Paula Filho et al., 2020) of the Parnaíba River Delta. Thus, carbon cycle studies in this area can provide key information to understanding the impact of global climate change on coastal ecosystems. However, to this date, there is no study focusing on the exchange of CO_2 between the estuary and the atmosphere, and how the river discharge would influence these fluxes.

In this context, this article presents the first direct measurements of CO_2 concentration and its fluxes, their spatial variability, as well as the primary biogeochemical processes that drive carbon behavior in the Parnaiba River Delta, during the rainy season. The hypothesis is that the CO_2 emissions of the Parnaíba river estuary are influenced by the river flow.

2. Methods

2.1. Study area

The Parnaíba river has a course of 1400 km from upstream to the ocean and forms the largest open sea delta in the Americas, with an area of 270,000 ha. The river basin covers 3,314,400 ha and it is divided into three sectors: high, medium, and low Parnaíba. The delta is important in the socio-economic development of the region, offering tourism potential and biodiversity richness. Although it is inserted in an environmental protection area, with low industrial development, the delta receives important anthropogenic pressure from the population of its drainage basin, mainly due to livestock farming, agriculture, and untreated domestic sewage (de Paula Filho et al., 2015).

The regional rainy period lasts from February to May, with 227.8 mm monthly average precipitation and maximum precipitation usually occurring in April (Fig. 1). The Intertropical Convergence Zone is the main atmospheric system driving the rainy season in this region, together with the occurrence and intensity of ENSO phenomena (Hastenrath, 2006). The variable discharge (Fig. 1) is a response to irregular rainfall. However, discharge values do not decrease lower than 100 $m^3\ s^{-1}$ due to the regulation by the Boa Esperança reservoir (around 700 km upstream from the Parnaíba river mouth).

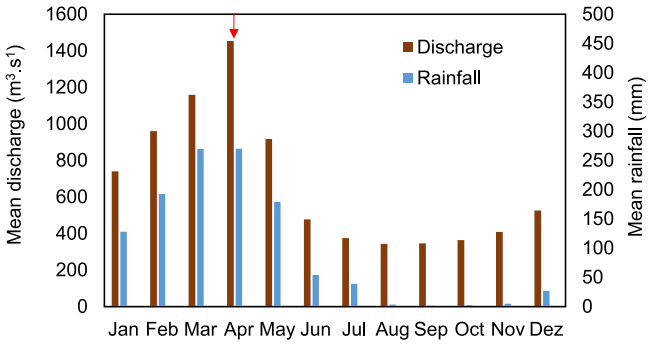

Fig. 1. Historical monthly average rainfall (1971–2017) and discharge (2014–2017) in Parnaíba region. Rainfall data from Parnaíba Station (OMM: 82287, INMET, 2017). Discharge data from Luzilândia station (SNIRH, 2017). Red arrow indicates when sampling campaign was performed.

2.2. Sampling strategy

Sampling was carried out in the main channel of the Parnaíba river delta, and in two of its secondary mangrove-dominated channels (Igarapé dos Periquitos and Tatus), during April/2017, the rainy season (Fig. 2). Continuous measurements of pCO_2, temperature, salinity, and wind velocity were taken by underway CO_2 equipment coupled with a thermosalinometer and an anemometer. While subsurface water samples were collected in 12 stations to analyze dissolved oxygen (DO), pH, total alkalinity (TA), dissolved organic carbon (DOC), carbon isotopic composition of DOC (δ13C), chlorophyll-*a* (Chl-*a*), and nutrients.

The DO and pH were measured *in situ* by a multiparametric probe (YSI® Professional Plus) and a Methrom® portable electrode (NBS scale), respectively.

2.3. Continuous measurements

Surface water temperature and salinity were measured using a Sea Bird thermo-salinometer. Wind speed and direction were recorded with an anemometer. Due to the interference of vessel movement, wind speed and direction were corrected using a vector decomposition.

The pCO_2 underway equipment function as described by Pierrot et al. (2009) and it was the one used in the studies of Carvalho et al. (2017), Cotovicz et al. (2020a) and Cotovicz et al. (2022) showing good accuracy and precision. The equipment comprises two showerhead equilibrators, an infrared analyser (LI-COR®, model LI-7000 CO_2/H_2O gas analyser), a GPS, and it is coupled to a thermo-salinometer and an anemometer. Computer software controls the system. The pressure measurements are within ± 0.2 mbars and the temperature within ±0.01 °C.

A calibration commanded separately is performed before starting the measurements using certified standards (360, 1009 and 2009 ppmv, White Martins Certified Material). Besides this calibration, every 6 h the system runs an automated one. Nitrogen is used as zero, free from CO_2 and water vapor. This procedure allows the accuracy of the pCO_2 measurements to be within ± 2 µatm (Pierrot et al., 2009). The CO_2 gas analyser (LI-COR Li7000) has a precision of 0.1 ppm with 1 min signal averaging (LI-COR, 2004).

Briefly, a flux of subsurface estuarine water is pumped to the equilibrators with a flux of 2.5–3.0 L min^{-1}. The air in equilibrium with the water from the equilibrators is dried and passes through a non-dispersive infrared analyser to measure the molar fraction of CO_2 (XCO_2^{eq}) in the estuarine water. The program records the following parameters every 5s: date and time, coordinates,

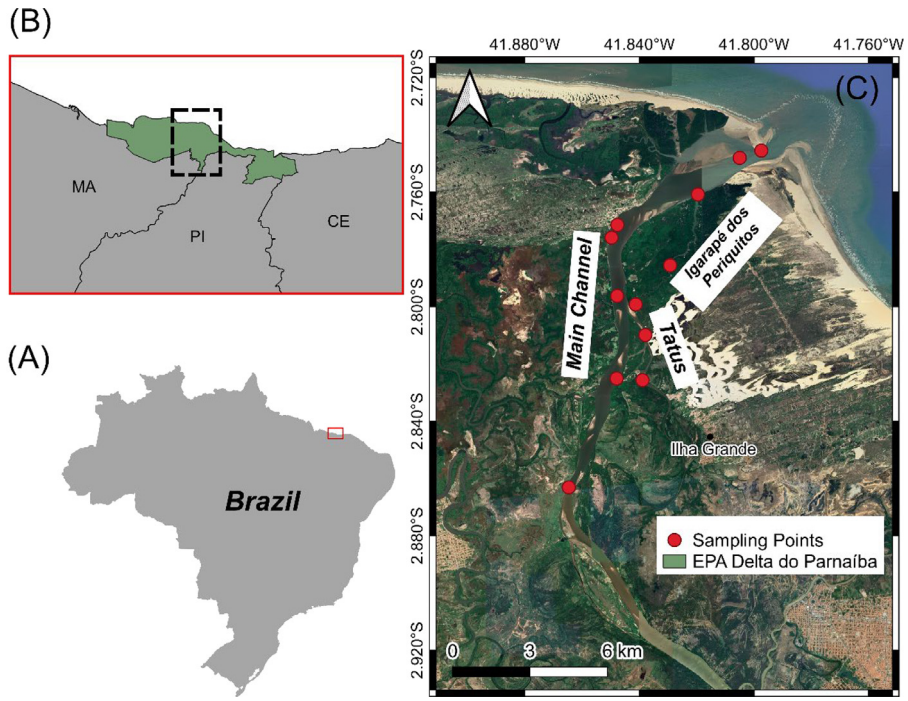

Fig. 2. Map of Parnaíba river estuary location in Brazil (A). The green area indicates the Environment Protection Area of the Parnaíba river Delta (B) and the red dots represent the sampling stations in April/2017 (C). (For interpretation of the references to color in this figure legend, the reader is referred to the web version of this article.)

velocity and route of the vessel, the XCO_2^{eq}, the water content in the detector, temperature, and salinity. Later, a 1 min average is made. The system also converts the XCO_2^{eq} into partial pressure of CO_2 (in μatm) in dry air, considering surface water temperature and 100% saturation of water vapor, according to (Weiss and Price, 1980):

$$pCO_2^{eq} = XCO_2^{eq} * (P_{eq} - P_w^{eq}), \quad (1)$$

where P_{eq} is the barometric pressure at equilibration and P_w^{eq} is the water vapor pressure (in atm) calculated at the equilibrator temperature. The accuracy of the pCO_2 measurements was estimated at about ± 2 μatm.

Takahashi et al. (2002) equation was used to convert the pCO_2 (μatm) in the equilibrator to the pCO_2 at the surface water temperature (SWT):

$$pCO_2^{sw} = pCO_2^{eq} * \exp^{[0.0423 * (SWT - Teq)]} \quad (2)$$

2.4. Laboratory analysis

Water samples for TA determination were sampled in duplicate in 500 mL borosilicate bottles, poisoned with 200 μL of a saturated solution of $HgCl_2$, sealed, stored cold, and protected from light. The TA measurements were performed by volumetric titration according to Standard Methods (APHA, 1999), using a standardized HCl 0.02N as titrant.

Dissolved organic carbon (DOC) samples were filtered *in situ* using 0.45 μm filters, stored in 120 mL amber bottles, and frozen until analysis. A HiperTOC Analyser was used to measure DOC in the sample. The method consists of the transformation of the dissolved carbon into CO_2 and its quantification in a non-dispersive infrared detector (Thermo, 2008).

Filtered water samples were pre-concentrated according to Dittmar et al. (2008) and the carbon isotopic composition of dissolved organic matter was measured using an elemental analyser Flash 2000 combined with the mass spectrometer Delta V Advantage (Thermo Scientific IRMS).

Samples for Chl-*a* and nutrient analysis were taken in 2L polypropylene bottles. The water was filtered, and dissolved nutrient samples were stored in amber bottles while the filter was stored protected from the light. Both water and filters were frozen until analysis. Total phosphorus (TP) measurements were made in unfiltered samples according to Valderrama (1981) method using spectrophotometry. Chlorophyll-*a* was extracted from filters using 90% ethanol and measured by a spectrophotometer according to Jeffrey and Humphrey (1975) equations. Trophic State Index (TSI) was obtained as a function of Chl-a and TP, according to Lamparelli (2004) equations.

2.5. Calculations

DIC was calculated from pCO_2, TA, water temperature, and salinity using the CO2SYS program (Lewis and Wallace, 1998). The dissociation constants for carbonic acid were those proposed by Merbach refitted by Dickson and Millero (1987) and the borate acidity constant by Lee et al. (2010).

The net estuary-air CO_2 fluxes (F, mmol m^{-2} d^{-1}) were calculated using:

$$F = k\ K_0(pCO_2^{water} - pCO_2^{atm}), \quad (3)$$

where K_0 is the solubility of CO_2 as a function of temperature and salinity (Weiss, 1974), pCO_2^{water} is the pCO_2 in the estuary and pCO_2^{atm} is the pCO_2 measured in the atmosphere, and k is the gas transfer velocity.

As *k* was not determined *in situ* and current velocity data was not available, we used wind speed estuary-specific parametrizations determined by Raymond and Cole (2001) (RC) and Borges et al. (2004) (BO), and Wanninkhof (2014) (WN) revised parametrization for open ocean waters:

$$k = 1.91 * \exp^{(0.35w)} * (600/Sc)^{-0.5} \quad (RC) \quad (4)$$

$$k = 5.141 * u^{0.758} * (600/Sc)^{-0.5} \quad (BO) \quad (5)$$

$$k = 0.251 * u^2 * (600/Sc)^{-0.5} \quad (WN) \quad (6)$$

where Sc represents the Schmidt number.

The apparent oxygen utilization (AOU, μmol kg^{-1}) was calculated according to Benson and Krause (1984), as following:

$$AOU = DO_{equilibrium} - DO_{in\ situ} \quad (7)$$

where, $DO_{equilibrium}$ represents the value of oxygen saturation concentration for the temperature and salinity measured and $DO_{in\ situ}$ represent the concentration of DO measured *in situ*.

The excess of CO_2 (E-CO_2, μmol kg^{-1}) was calculated according to (Abril et al., 2000)

$$E - CO_2 = DIC_{in\ situ} - DIC_{equilibrium} \quad (8)$$

where, $DIC_{in\ situ}$ is the concentration of DIC at *in situ* conditions and $DIC_{equilibrium}$ represents the DIC calculated from the observed TA and the pCO_2 values assuming equilibrium between the aquatic and atmospheric CO_2 concentrations (407 μatm) using the CO2SYS software.

2.6. Conservative mixing lines

The conservative mixing of TA and DIC were estimated according to (Jiang et al., 2008):

$$C_{mixing} = (S_i/S_{ocean}) * C_{ocean} + (1 - S_i/S_{ocean}) * C_{river} \quad (9)$$

where Si is the salinity in the sampling station, Socean the salinity in the ocean endmember and Sriver the salinity in the riverine endmember; the Cocean is the variable concentration in the ocean endmember and Criver the concentration in the riverine endmember. The CO_2 mixing curve was then estimated according to the DICmixing and TAmixing values through the CO2SYS program (Lewis and Wallace, 1998), using the corresponding average temperature and the constants stated before.

2.7. River discharge estimation

The Parnaíba river flow was determined from the historical average discharge data provided by the Agência Nacional de Águas (ANA) and the instantaneous flow measurements done by an Acoustic Doppler Profiler (ADCP) with 1.5 MHz frequency, manufactured by SONTEK/YSI (Dias et al., 2016; dos Santos et al., 2020; Lima et al., 2021).

The fluvial flows (Qf) were obtained in the cross-sections to the average flux of the area A = A(x,z) along the Parnaíba River Estuary, and calculated by numeric integration:

$$Qf = \frac{1}{T}\int_0^T \left[\frac{1}{A}\iint_A \vec{v}.\vec{n}\,.dA\right] dt, \quad (10)$$

where: $\vec{v} = \vec{v}(x, z, t)$ is the velocity vector; $\vec{n}$ is the normal verse to section A; t is the sampling instant; x is the horizontal distance of the section; z is the depth. This physical parameter was calculated in International System units ($m^3\ s^{-1}$).

Considering the measured *in situ* discharge, P1 was determined as the contribution point of the freshwater volume from the drainage basin to the estuary. Based on these data, an estimate of the percentage of gain and loss in the ebbing and flooding tides was performed. Based on these percentages, the historical average flow rate was calculated for the month of April 2017 (ANA), the sampling period with tidal height, and considering the type of tide in this period (da Silva Dias et al., 2011).

2.8. Riverine CO_2 contribution to estuarine emissions

The contribution of CO_2 originating from within the estuarine zone and from the river was estimated to evaluate the relative contribution of riverine water in the overall estuarine CO_2 dynamics. The relative contribution of the riverine CO_2 to the overall emissions in the estuary was calculated (Rosentreter et al., 2018):

$$\text{Riverine contribution } (\%) = (F_{River}/F_{Estuary}) * 100, \quad (11)$$

where F_{River} is the riverine CO_2 flux to the estuary calculated from the estimated river discharge and riverine excess CO_2 (in mol d^{-1}) (Borges et al., 2006). The riverine excess CO_2 was calculated following Eq. (8), with $DIC_{in\ situ}$ as the DIC at the river endmember. $F_{estuary}$ is the average estuarine flux to the atmosphere (mol d^{-1}) (from Eq. (3)).

2.9. Statistical analysis

Data normality was verified by the Shapiro–Wilk test. As data did not present normal distribution, non-parametric tests were performed. We used Spearman's rank correlation coefficient to investigate the correlation between variables, and differences between channels were assessed by the Kruskal–Wallis test. A Principal Component Analysis was made to identify patterns and processes in the dataset. All statistical analyses were based on $\alpha = 0.05$.

3. Results

The average, standard deviation, and range of temperature, salinity, pCO_2, wind speed, and air–water CO_2 fluxes are displayed in Table 1. The estimated fluvial discharge of 10 days before sampling was 519.13 $m^3\ s^{-1}$, lower than the historical average outflows for the month. Nevertheless, salinity in the estuary was low, ranging from 0.04 to 26.37. Maximum values were found near the river mouth, during flood tide. Thus, a great variation of salinity was found in the main channel of the river and in the tidal channel near the river mouth. Water temperature was high and with low variation, with an average of 30.83 ± 0.27 °C. The mean wind speed was 5.01 ± 2.38 m s^{-1}, however, the wind speed was significantly lower (p-$value < 0.01$) inside the tidal channels. The estuarine pCO_2 ranged from 390 to 5539 μatm, with significant differences between main and tidal channels (p-$value < 0.01$). The tidal channels had the highest mean pCO_2 (Igarapé = 3034 ± 1815 μatm and Tatus = 3303 ± 641 μatm), while the main channel exhibited the lowest mean values (1766 ± 608 μatm).

Considering all the parametrizations used, the CO_2 flux from the Parnaíba river estuary to the atmosphere ranged from −3.9 to 1131.8 mmol $m^{-2}\ d^{-1}$ (Table 1). There were significant differences according to the gas transfer velocity used (p-$value < 0.01$). On average, fluxes calculated using Wanninkhof's 2014 parametrization were the lowest, while the fluxes calculated using Borges et al. (2004) parametrization were the highest. Also, significant differences (p-$value < 0.01$) between the three channels sampled were found. The main channel was, in general, the area with higher fluxes. It was estimated that the riverine CO_2 contributed to around 73% of the overall CO_2 emissions in the main channel of the estuary.

The DO values ranged from 4.26 to 6.88 mg L^{-1} with lower DO occurring in the Tatus channel. The average Chl-*a* value was 13.11 ± 6.19 μg L^{-1}. The minimum values occurred near the river mouth (Min = 3.53 μg L^{-1}), while the main channel was the area with the highest levels (Max = 23.0 μg L^{-1}). The TP concentrations ranged between 0.29 μM and 0.77 μM (mean = 0.46 ± 0.13 μM). On average the main channel presented higher TP concentrations. Minimum values occurred in high salinity areas and the tidal channels presented lower TP values. According to the Chl-a and TP values found and using the Lamparelli index, the estuary was in general an eutrophic environment.

Table 1
Descriptive values of the variables measured continuously in the Parnaíba river estuary, including all channels sampled and subdivisions between the main channel of the river and the secondary channels (Igarapé dos Periquitos and Tatus).

		Temperature (°C)	Salinity	pCO_2 (μatm)	Wind Speed (m s^{-1})	$Flux_{BO}$[a]	$Flux_{RC}$[a]	$Flux_{WN}$[a]
						(mmol m^{-2} day^{-1})		
All *(n = 696)*	Mean	30.83	2.46	2196	5.01	262.8	215.9	103.9
	SD	0.27	6.39	1095	2.38	144.8	197.5	93.8
	Min	30.17	0.04	390	0.35	−3.4	−3.9	−2.1
	Max	31.37	26.37	5539	11.23	714.0	1131.8	510.2
Main Channel *(n = 485)*	Mean	30.85	3.00	1766	5.89	242.4	241.1	120.0
	SD	0.25	7.15	608	2.22	131.5	223.5	101.7
	Min	30.17	0.04	390	0.49	−3.4	−3.9	−2.1
	Max	31.29	26.37	3866	11.23	677.5	1131.8	510.2
Igarapédos Periquitos *(n = 93)*	Mean	30.96	2.57	3034	2.60	259.2	121.4	42.0
	SD	0.28	5.56	1815	1.04	192.1	89.1	39.6
	Min	30.17	0.09	435	0.35	2.3	1.0	0.3
	Max	31.37	25.07	5539	6.20	627.3	321.4	161.9
Tatus *(n = 118)*	Mean	30.66	0.15	3303	3.31	349.7	186.8	86.1
	SD	0.25	0.14	641	1.33	119.4	89.7	61.3
	Min	30.42	0.04	1173	0.36	85.4	39.7	1.2
	Max	31.17	0.72	4795	6.74	714.0	660.4	372.7

[a]Estuary–atmosphere fluxes calculated according to parametrizations determined by Raymond and Cole (2001) (RC), Borges et al. (2004) (BO), and Wanninkhof (2014) (WN).

The carbonate system variables (TA, pH, and DIC) in the Parnaíba river estuary were also higher near the river mouth, with the increasing salinity. The TA, in freshwater zones, ranged from 328.3 to 473.2 μmol kg^{-1}, while in higher salinity waters TA varied from 1759.45 to 1880.20 μmol kg^{-1}. The pH showed lower variation (mean = 7.09 ± 0.36) whereas mean DIC concentration was 672.56 ± 447.90 μM with maximum values also occurring near river mouth (Max = 1725.97 μM).

The mean DOC concentrations were 370.53 ± 160.37 μM. The main channel presented the highest DOC concentrations, while minimum values occurred in higher salinity waters, as expected in estuarine areas due to flocculation and deposition of organic matter. Also, light δ^{13}C-DOC (−27.77 ± 0.40 ‰) values predominated along the estuary.

4. Discussion

4.1. pCO_2 spatial variability and drivers

The significant differences in pCO_2 between the channels indicate a strong spatial variability in the study area (Fig. 3). Overall, most of the pCO_2 values were above atmospheric equilibrium at that time (407 μatm), while lower concentrations were restricted to higher salinity areas. Although salinities higher than 1 occurred inside the Igarapé channel during flood tide, pCO_2 was not as low as in the main channel. In fact, maximum CO_2 values were found in this channel, which is consistent with other estuaries surrounded by mangrove forests, where mangrove channels usually have higher CO_2 concentrations than the associated estuary (Borges et al., 2003).

As the sampling campaign was carried out during the rainy period, freshwater was observed throughout the inner channels down to near the river mouth, where saline intrusion occurred only during high tide. Thus, the salinity gradient was only present near the river mouth advancing towards the ocean. Even though pCO_2 had a low, but significant, inverse correlation ($r = -0.17$, $p < 0.05$) with salinity, and its variation relative to the salinity followed a near-conservative pattern (Fig. 4), mainly in the main river channel, with decreasing values with increasing salinity.

The pCO_2 values lower than the atmospheric equilibrium were found in the main channel and are probably related to the mixing of river and seawater. The low buffering capacity of freshwaters in the delta, where we found a river end-member TA of 328.30 μmol kg^{-1}; together with carbonate thermodynamics can be the predominant driver of pCO_2 variability and generate this CO_2 undersaturation along the mixing zone, as it was observed in other tropical river estuaries (Abril et al., 2021; Cotovicz et al., 2020b). The higher values in the upper-estuarine zone are consistent with other studies (Chen et al., 2013) and are mainly due to the entrance of the CO_2-enriched fluvial waters.

Whether the carbon emitted from the estuary derives from the estuary (autochthonous) or from outside (allochthonous) has implications for coastal carbon budgets. According to Borges et al. (2006), it was estimated that riverine CO_2 would contribute to around 10% of the total estuary emission and that this contribution is controlled mainly by the water residence time of the estuary. In this study, the estimated ventilation of river-born CO_2 contributes to around 73% of CO_2 emission in the Parnaíba estuary. This indicates that this riverine CO_2 is fully ventilated to the atmosphere within the estuary, and the 27% remaining is derived from the net heterotrophy of the estuary itself or another external carbon source (Rosentreter et al., 2018).

In the case of the Parnaiba estuary, the results indicate that this flux is fueled by the respiration of organic matter brought by the river, which has a significant impact on the magnitude of the organic matter taken to the estuary and its residence time. These two processes are key for the modification of organic matter in the estuary and the formation of CO_2. The light δ^{13}C-DOC values found (−27.77 ± 0.40 ‰) and higher DOC values in the main channel indicate a strong transfer of superior plants' organic matter by the river to the estuarine system. In addition, there is a contribution of the mangrove forest in the estuarine region that provides a new organic matter, part refractory and part a young matter as has been observed in estuaries in the region (Mounier et al., 2018). Still, the Chl-*a* values within the freshwater zone (salinity <1) were significantly correlated with DO ($r = 0.93$, $p < 0.01$) and inversely with pCO_2 ($r = -0.80$, $p < 0.01$), pointing to the significative presence of primary production in the estuary (Fig. 6). In fact, the δ^{13}C-DOC values found can be related to a mixing of sources, such as C3 litter and soils from terrestrial sources, but also from freshwater phytoplankton (Cavalcante et al., 2021). Riverine and estuarine plankton can have a wide span of stable carbon isotopic compositions (<22 < δ13C< −28‰; Fry and Sherr (1989)) that can be masked by the C3 plant signal.

Although the estuary was considered well-oxygenated as no values were lower than 4 mg L^{-1} (de Assis Esteves, 1998), DO levels were below saturation in the study area. Minimum values

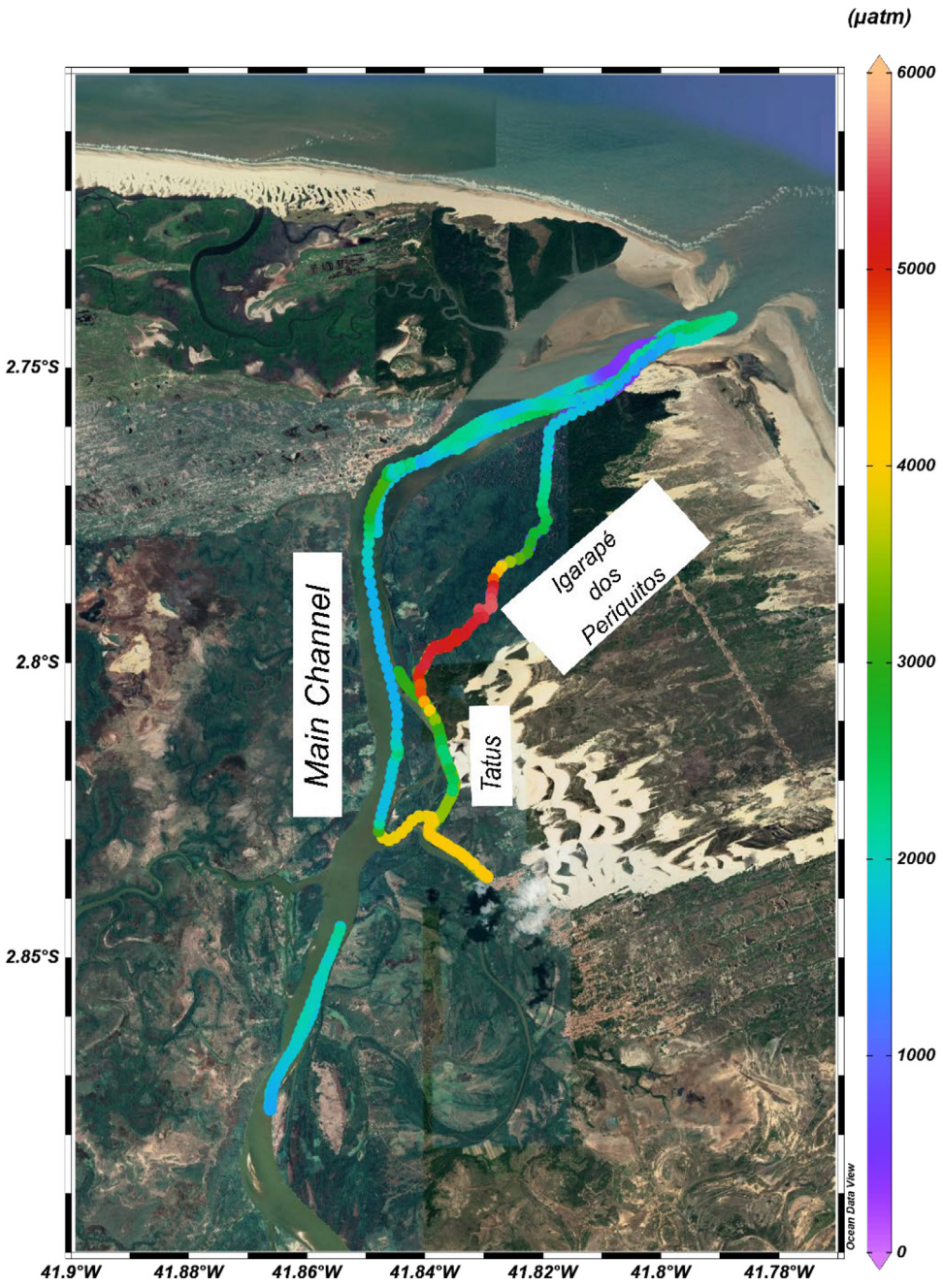

Fig. 3. Spatial distribution of pCO_2 (in µatm) along the different channels sampled in the Parnaíba river estuary in the rain season, April 2017.

were found together with maximum pCO_2 values as DO and pCO_2 were significantly and inversely correlated ($r = -0.85$, $p < 0.01$) (Fig. 6b), indicating that both are controlled by the same processes: mineralization and photosynthesis. The positive AOU values together with the excess of CO_2 (Fig. 5), indicate that O_2 consumption is linked to CO_2 production through the respiration of organic matter (Zhai et al., 2005).

Due to the presence of more developed mangroves, the tidal channels presented lower TP values, as this kind of vegetation can retain phosphorus from the water column depending on forest health (Marins et al., 2020; Sánchez-Carrillo et al., 2009). The general trophic state of the estuary is eutrophic, however, the intrusion of seawater during flood tide promotes a shift in the trophic status in higher salinity areas, turning it into mesotrophic.

A Principal Component Analysis including all sampling points and all variables analyzed in this study (Fig. 7a) returned two components that accounted for a cumulative percentage of the variance of 82.37% (PC1 = 60.96% and PC2 = 21.41%). PC1 seemed to represent the shift between fresh and salt waters, as positive PC1 values represented higher values of salinity, TA, DIC, and pH, associated with the higher salinity stations, when flood tide occurred. The PCA within freshwater stations (Fig. 7b) also returned two main components accounting for 81.02% of the cumulative percentage of the variance. PC1 (50.14%) appeared to represent the difference between the main channel and tidal channels, as negative values reported the stations among the main channel, whereas positive values account for both secondary channels sampled. The main channel stations are represented by higher values of DOC, Chl-*a*, and DO, while Tatus channel presented maximum pCO_2, and mangrove channel (Igarapé dos Periquitos) had higher DIC, TA and pH. The opposing relationship between pCO_2

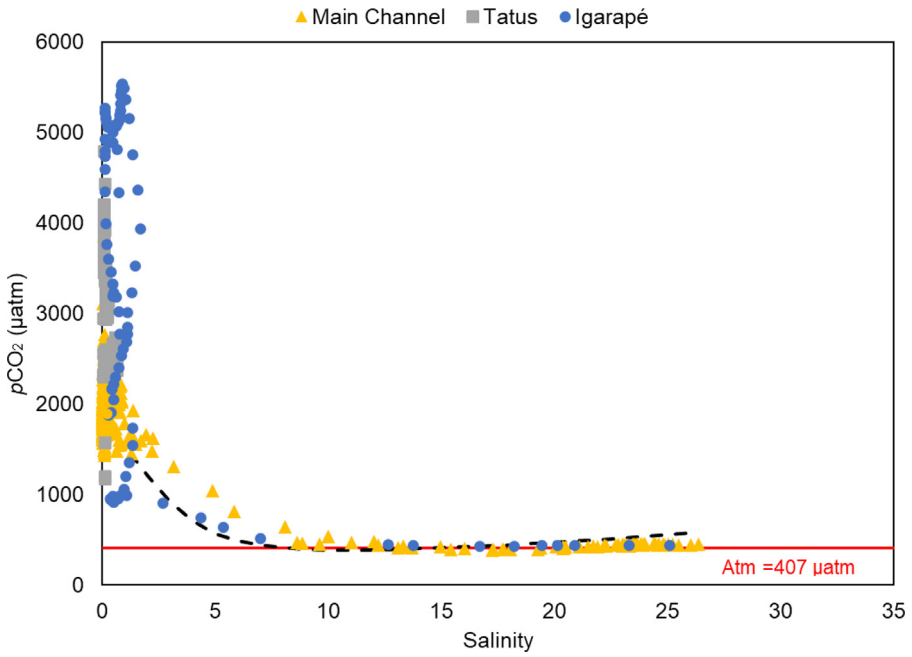

Fig. 4. Distribution of surface water pCO_2 against salinity. Different colors indicate the different channels sampled (yellow triangle — main channel; gray square — Tatus channel; blue circle — Igarapé dos Periquitos). Dashed black line indicates conservative mixing. Solid red line represents atmospheric value.

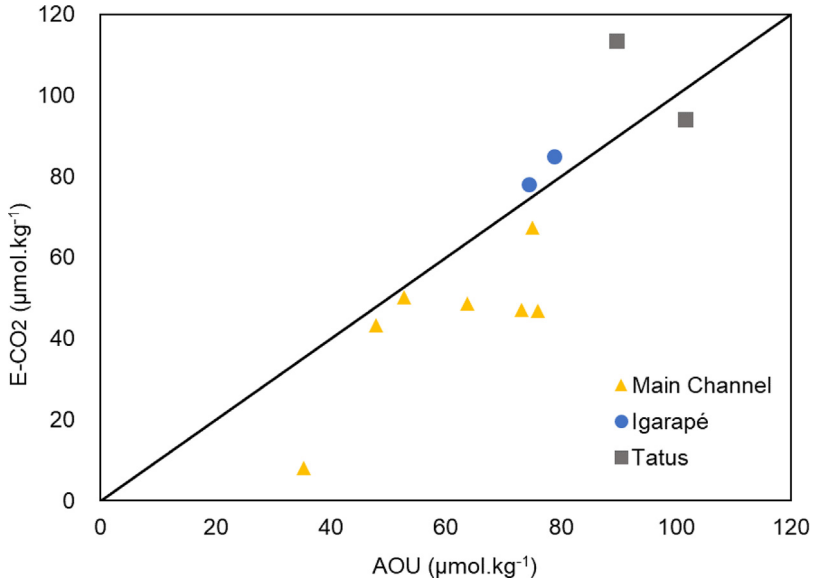

Fig. 5. Excess CO_2 vs. Apparent Use of Oxygen in the Parnaíba river estuary, for the channels sampled (yellow triangles = main channel; blue circles = mangrove channel (Igarapé dos Periquitos); and gray squares = Tatus channel). The 1:1 line represents the quotient between CO_2 and O_2 during the processes of photosynthesis and respiration.

and DO and Chl-*a* highlights the presence of primary production in the estuary.

The relatively high CO_2 levels of the study area are likely controlled by a combination of factors that may differ among the different channels sampled. The sampled biogeochemical variables and the PCA showed distinct spatial patterns, with a clear influence of two processes: fluvial and marine. The seawater intrusion promoted a dilution of the riverine water, while organic matter respiration and primary production were dominant along freshwater zones of the main and tidal channels. In addition, the increase in pCO_2 along mangrove-dominated channels shows that these systems are an important source of carbon to the estuary.

4.2. CO_2 fluxes to the atmosphere

The issue of using wind, or wind speed, models from data from distant weather stations are not usually addressed in flux calculations. In this study, wind speed varied significantly between the channels sampled (Fig. 8). The tidal channels can be considered a wind-protected environment due to the mangrove forest, thus, the mean wind speed was significantly lower ($p < 0.01$). This may have caused lower average CO_2 fluxes in these channels, since, in general, even with higher pCO_2, they had lower fluxes than the main channel.

The selection of a gas transfer velocity is also a problem in accessing the CO_2 global flux of estuaries. As shown in this study and others (Call et al., 2014; Rosentreter et al., 2018) there are

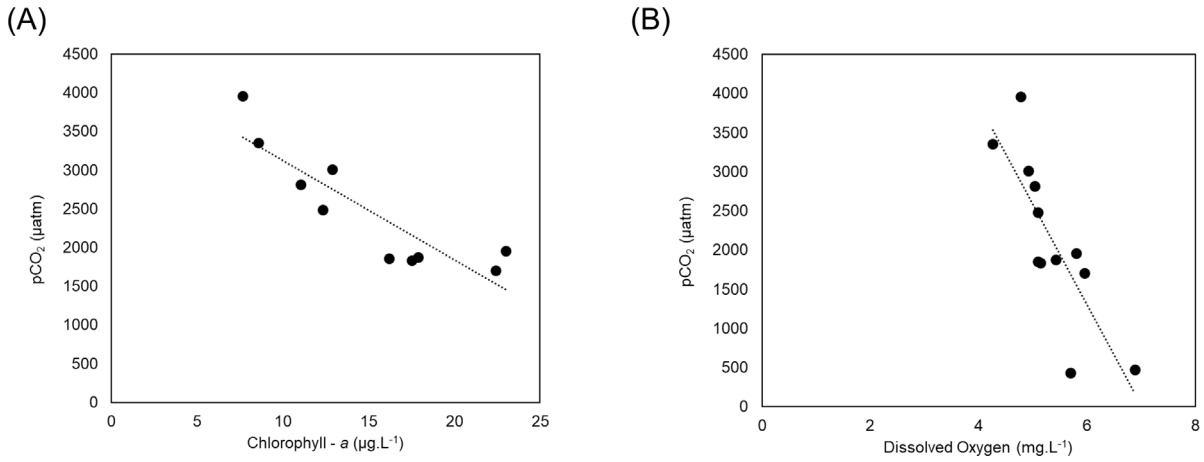

Fig. 6. (a) Estuarine pCO_2 against Chl-*a* in freshwaters (S < 1) stations. Spearman correlation coefficient r = −0.80 (p < 0.01). (b) Estuarine pCO_2 against DO in all stations. Spearman correlation coefficient r = −0.85 (p < 0.01).

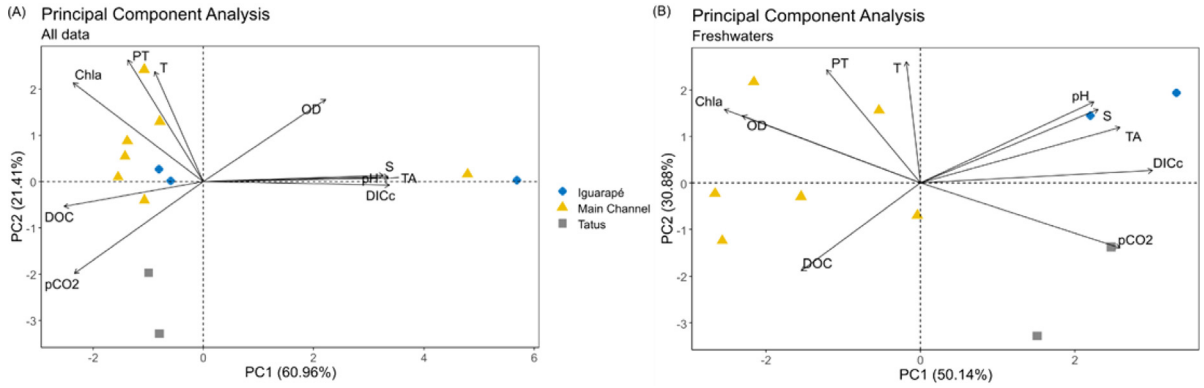

Fig. 7. Principal Component Analysis using all sampling points (a) and only in freshwater stations (b). Main channel stations are represented in yellow triangles, Tatus channel in gray squares and Igarapé dos Periquitos channel in blue dots.

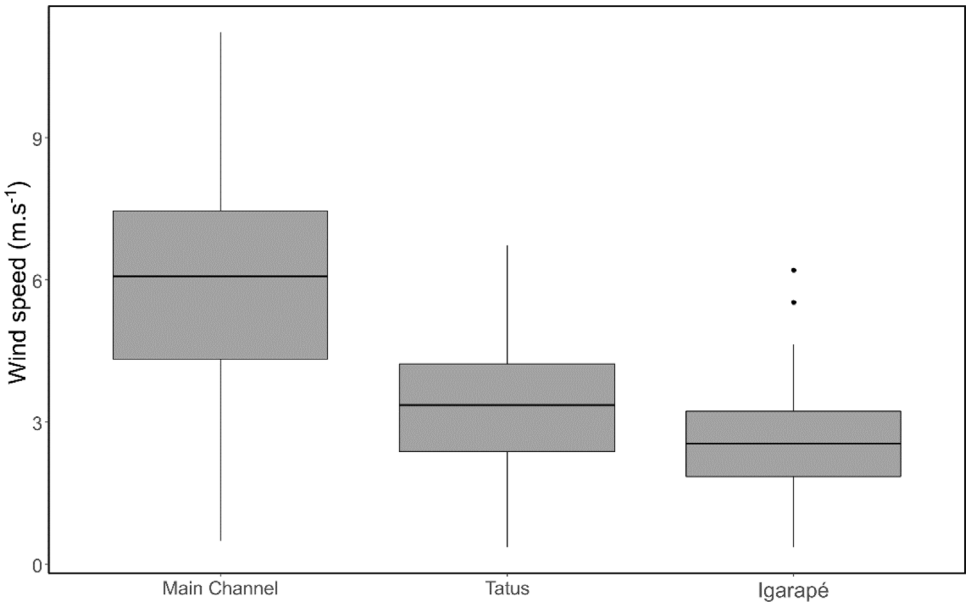

Fig. 8. Boxplot of wind speed (m s^{-1}) variation according to the channels sampled in the Parnaíba river estuary, in the rain season, April 2017.

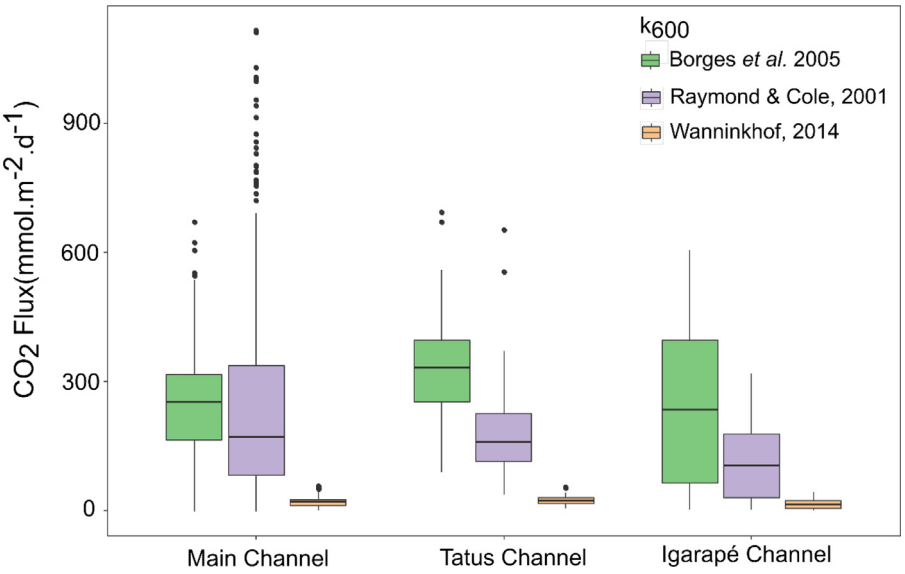

Fig. 9. Boxplot of the CO_2 fluxes to the atmosphere (mmol C m^{-2} d^{-1}) in each channel sampled in the Parnaíba river estuary according to the k_{600} used: Borges et al., 2005 (green), Raymond and Cole (2001) (magenta) and Wanninkhof (2014) (orange). (For interpretation of the references to color in this figure legend, the reader is referred to the web version of this article.)

significant differences in the calculation of the fluxes according to the *k* chosen (Fig. 9). Therefore, the decision of the proper *k* may imply underestimating or overestimating fluxes. The best model for k in estuarine environments is still a matter of discussion and outside the scope of this study. Thus, the fluxes in this study were determined using three different models.

The average flux of CO_2 found using the 3 models ranged from −3.9 to 1131.8 mmol C m^{-2} d^{-1} (average flux 194.2 ± 135.2 mmol C m^{-2} d^{-1}). The spatial variability found in pCO_2 was reflected in the flux, resulting in a large standard deviation. However, the lower wind speed in the tidal channels may have adjusted the fluxes. The lower emissions, sometimes reaching negative values, were due to the seawater intrusion in the main and Igarapé channels during flood tide.

The mean flux of the Parnaíba river estuary for this season is more than 100% higher than the revised global estimate for estuaries between 0–23.5°S (52.1 ± 16.1 mmol m^{-2} d^{-1}) by Rosentreter et al. (2018). The average flux calculated using Wanninkhof (2014) parametrization (103.9 ± 93.8 mmol C m^{-2} d^{-1}) was the only one near the range suggested for southern tropical global estuarine emissions (44.1 ± 29.3 mmol m^{-2} d^{-1}) estimated by Chen et al. (2013). The mangrove-dominated channel (Igarapé dos Periquitos) presented fluxes as high as those found in some estuarine mangrove creeks (Call et al., 2014; Borges et al., 2018; Rosentreter et al., 2018), but still falls above the average of CO_2 fluxes compiled globally by Rosentreter et al. (2018). This highlights how heterogenous estuaries are, and the need for more studies in these tropical systems.

5. Conclusions

This study reports the first spatial distribution of pCO_2 and its fluxes in the Parnaíba river delta in Brazil, and the drivers for its behavior. Although classified as dominated by waves and tides, the results suggest a strong influence of the river discharge in the delta main channel, responding to the values observed in the Parnaíba river region, especially during the rainy season with high discharge, and explaining the shift of pCO_2 previously observed in this transitional zone of the Brazilian equatorial continental shelf. The large contribution of riverine-CO_2 to estuary emissions, together with the light isotopic composition of dissolved carbon indicates that the river carbon input fueled the CO_2 emissions in this estuary. In addition, chlorophyll-a values revealed the contribution of the primary productivity to the carbon dynamics in the delta, however, the freshwater phytoplankton isotopic signal may have been masked, suggesting the need to use additional techniques to evaluate the carbon origin in this type of ecosystem. The primary production together with the respiration of organic matter controlled the CO_2 variability in the river's main and secondary channels, while seawater dilution controlled the biogeochemical behavior near the river mouth. The estuary was supersaturated in CO_2 with values ranging from 390 to 5539 μatm and behaved as a strong source of this gas to the atmosphere with the mean flux using different gas transfer models ranging from −3.9 to 1131.8 mmol m^{-2} d^{-1} during the study period. This flux was higher than recent global estimates for estuaries in the southern tropics but similar to those found in some estuaries and mostly in mangrove-dominated systems. The results also show how important is the marine intrusion to sequester organic matter, and decrease the CO_2 fluxes significantly, in this Brazilian equatorial coastal system. This process is probably strengthened in the dry season. This study offers the first estimate of CO_2 fluxes in the largest open sea delta in Americas and highlights the great spatial variability and heterogeneity of coastal systems, and it hopes to improve the precision of global CO_2 emission estimates in a climate change scenario.

CRediT authorship contribution statement

R.S.A. Chielle: Formal analysis, Investigation, Writing – original draft. **R.V. Marins:** Conceptualization, Resources, Writing – review & editing, Project administration, Funding acquisition. **F.J.S. Dias:** Investigation, Software. **K.K. Borges:** Investigation. **C.E. Rezende:** Investigation, Resources.

Declaration of competing interest

The authors declare that they have no known competing financial interests or personal relationships that could have appeared to influence the work reported in this paper.

Data availability

Data will be made available on request.

Acknowledgments

This study was financed by the Fundação Cearense de Apoio ao Desenvolvimento Científico e Tecnológico (FUNCAP), Brazil, Program PRONEX/CNPq (Proc. No. PR 2-0101-0052.01.00/2015). Rozane V. Marins thanks the CNPq, Brazil/ Proc. No. 309718/2016-3; Raisa S A Chielle thanks the FUNCAP, Brazil for the Ph.D. grant; and Carlos Eduardo de Rezende thanks the CNPq, Brazil/ Proc. 305217/2017-8 and FAPERJ, Brazil NºE-26/202.916/2017.

References

Gattuso, J.-P., Frankignoulle, M., Wollast, R., 1998. Carbon and carbonate metabolism in coastal aquatic ecosystems. Annu. Rev. Ecol. Syst. 29, 405–434.

Borges, A.V., Abril, G., 2011. Carbon dioxide and methane dynamics in estuaries. In: Treatise on Estuarine and Coastal Science. p. 10812. http://dx.doi.org/10.1016/B978-0-12-374711-2.00504-0.

Le Quéré, C., Andrew, R.M., Friedlingstein, P., Sitch, S., Hauck, J., Pickers, P., Korsbakken, J.I., Peters, G.P., Canadell, J.G., Arneth, A., Arora, V.K., Barbero, L., Bastos, A., Bopp, L., Chini, L.P., Ciais, P., Doney, S.C., Gkritzalis, T., Goll, D.S., Harris, I., Haverd, V., Hoffman, M., Hoppema, M., Houghton, R.A., Ilyina, T., Jain, A.K., Johannesen, T., Jones, C.D., Kato, E., Keeling, R.F., Goldewijk, K.K., Lienert, S., Lombardozzi, D., Metzl, N., Munro, D.R., Nakaoka, S., Neill, C., Olsen, A., Ono, T., Patra, P., Peregon, A., Peters, W., Peylin, P., Pfeil, B., Pierrot, D., Poulter, B., Resplandy, L., Robertson, E., Rocher, M., Schuster, U., Skjelvan, I., Steinhoff, T., Sutton, A., Pieter, P., Tian, H., Tilbrook, B., Tubiello, F.N., Laan-luijkx, I.T., Van Der, Guido, R., Werf, V. Der, Viovy, N., Walker, A.P., Wiltshire, A.J., Wright, R., Sciences, P., Sciences, A., Project, G.C., Canada, C.C., Studies, A., Science, A., Oceanic, N., Quéré, C.Le., Andrew, R.M., Friedlingstein, P., Sitch, S., Hauck, J., Pongratz, J., Pickers, P., Korsbakken, J.I., Peters, G.P., Canadell, J.G., 2018. Global carbon budget 2018. Earth Syst. Sci. Data 10, 1–3. http://dx.doi.org/10.5194/essd-10-2141-2018.

Bauer, J.E., Cai, W.-J., Raymond, P.A., Bianchi, T.S., Hopkinson, C.S., Regnier, P.A.G., 2013. The changing carbon cycle of the coastal ocean. Nature 504, 61–70.

Borges, A.V., Abril, G., Bouillon, S., 2018. Carbon dynamics and CO 2 and CH 4 outgassing in the mekong delta. Biogeosciences 15, 1093–1114.

Sarma, V., Viswanadham, R., Rao, G.D., Prasad, V.R., Kumar, B.S.K., Naidu, S.A., Kumar, N.A., Rao, D.B., Sridevi, T., Krishna, M.S., et al., 2012. Carbon dioxide emissions from Indian monsoonal estuaries. Geophys. Res. Lett. 39.

Sawakuchi, H.O., Neu, V., Ward, N.D., Barros, M. de L.C., Valerio, A.M., Gagne-Maynard, W., Cunha, A.C., Less, D.F.S., Diniz, J.E.M., Brito, D.C., et al., 2017. Carbon dioxide emissions along the lower amazon river. Front. Mar. Sci. 4 (76).

Carvalho, A.C.O., Marins, R.V., Dias, F.J.S., Rezende, C.E., Lefèvre, N., Cavalcante, M.S., Eschrique, S.A., 2017. Air-sea CO 2 fluxes for the Brazilian northeast continental shelf in a climatic transition region. J. Mar. Syst. 173, 70–80.

Abril, G., Borges, A.V., 2004. Carbon dioxide and methane emissions from estuaries. In: Greenhouse Gas Emissions—Fluxes and Processes. Springer, pp. 187–207.

Chen, C.-T., Huang, T.-H., Chen, Y.-C., Bai, Y., He, X., Kang, Y., 2013. Air–sea exchanges of CO 2 in the world's coastal seas. Biogeosciences 10, 6509–6544.

Laruelle, G.G., Lauerwald, R., Pfeil, B., Regnier, P., 2014. Regionalized global budget of the CO2 exchange at the air–water interface in continental shelf seas. Glob. Biogeochem. Cycles 28, 1199–1214.

Ovalle, A.R.C., Rezende, C.E., Lacerda, L.D., Silva, C.A.R., 1990. Factors affecting the hydrochemistry of a mangrove tidal creek, sepetiba bay, Brazil. Estuar. Coast. Shelf Sci. 31, 639–650. http://dx.doi.org/10.1016/0272-7714(90)90017-L.

Souza, M.F.L., Gomes, V.R., Freitas, S.S., Andrade, R.C.B., Knoppers, B., 2009. Net ecosystem metabolism and nonconservative fluxes of organic matter in a tropical mangrove estuary, piauí river (NE of Brazil). Estuar. Coasts 32, 111–122. http://dx.doi.org/10.1007/s12237-008-9104-1.

Cotovicz, Jr., L.C., Knoppers, B.A., Brandini, N., Costa Santos, S.J., Abril, G., Cotovicz, L.C., Knoppers, B.A., Brandini, N., Costa Santos, S.J., Abril, G., Cotovicz, Jr., L.C., Knoppers, B.A., Brandini, N., Costa Santos, S.J., Abril, G., 2015. A large CO2 sink enhanced by eutrophication in a tropical coastal embayment (Guanabara Bay, Rio de Janeiro, Brazil). Biogeosci. Discuss 12, 4671–4720.

Marotta, H., Peixoto, R.B., Fonseca, T., Peruzzi, V., Costa, R., Keim, R., Musetti, C.A., Cotrim, L., Moser, G., Pollery, R.C., Pinho, L., 2020. BIOMONITORAMENTO CONTÍNUO DE ÁGUAS DO PELD-BAÍA DE GUANABARA: INTENSA VARIAÇÃO NICTEMERAL DE GASES METABÓLICOS NA CONDIÇÃO EUTRÓFICA TROPICAL. Oecol. Aust. 24 (2), http://dx.doi.org/10.4257/oeco.2020.2402.10, Article 2.

Cotovicz, Jr., L.C., Marins, R.V., da Silva, A.R.F., 2022. Eutrophication amplifies the diel variability of carbonate chemistry in an equatorial, semi-arid, and Negative Estuary. Front. Mar. Sci. 9.

Call, M., Santos, I.R., Dittmar, T., de Rezende, C.E., Asp, N.E., Maher, D.T., 2019. High pore-water derived CO2 and CH4 emissions from a macro-tidal mangrove creek in the Amazon region. Geochim. Cosmochim. Acta 247, 106–120. http://dx.doi.org/10.1016/J.GCA.2018.12.029.

Grazielle, M., Portela, T., Mira, G., Amorim, A., Souza, G., Joa, V., 2020. Vegetation Biomass and Carbon Stocks in the Parnaíba River Delta, NE Brazil. Wetlands Ecol Manage, 0123456789. http://dx.doi.org/10.1007/s11273-020-09735-y.

Aquino da Silva, A.G., Stattegger, K., Vital, H., Schwarzer, K., 2019. Coastline change and offshore suspended sediment dynamics in a naturally developing delta (parnaíba delta, NE Brazil). Mar. Geol. 410, 1–15. http://dx.doi.org/10.1016/j.margeo.2018.12.013.

da Silva, A.G.A., Stattegger, K., Schwarzer, K., Vital, H., Heise, B., 2015. The influence of climatic variations on River Delta hydrodynamics and morphodynamics in the Parnaiba Delta, Brazil. J. Coast. Res. 31, 930–940.

Ferreira, T.A.B., Aquino da Silva, A.G., Reyes Perez, Y.A., Stattegger, K., Vital, H., 2021. Evaluation of decadal shoreline changes along the Parnaíba Delta (NE Brazil) using satellite images and statistical methods. Ocean Coast. Manag. 202, http://dx.doi.org/10.1016/j.ocecoaman.2020.105513.

Paula Filho, F.J., Marins, R.V., Chicharo, L., Souza, R.B., Santos, G.V., Braz, E.M.A., 2020. Evaluation of water quality and trophic state in the parnaíba River Delta, northeast Brazil. Reg. Stud. Mar. Sci. 34, 101025. http://dx.doi.org/10.1016/j.rsma.2019.101025.

de Paula Filho, F.J., Marins, R.V., de Lacerda, L.D., 2015. Natural and anthropogenic emissions of N and P to the Parnaíba River Delta in NE Brazil. Estuar. Coast. Shelf Sci. 166, 34–44. http://dx.doi.org/10.1016/j.ecss.2015.03.020.

Hastenrath, S., 2006. Circulation and teleconnection mechanisms of northeast Brazil droughts. Prog. Oceanogr. 70, 407–415. http://dx.doi.org/10.1016/j.pocean.2005.07.004.

INMET, http://www.inmet.gov.br/portal/index.php?r=bdmep/bdmep.

SNIRH, http://www.snirh.gov.br/hidroweb/publico/apresentacao.jsf.

Pierrot, D., Neill, C., Sullivan, K., Castle, R., Wanninkhof, R., Lüger, H., Johannessen, T., Olsen, A., Feely, R.A., Cosca, C.E., 2009. Recommendations for autonomous underway pCO 2 measuring systems and data-reduction routines. Deep Sea Res. II 56, 512–522.

Cotovicz, Jr., L.C., Chielle, R., Marins, R.V., 2020a. Air-sea CO2 flux in an equatorial continental shelf dominated by coral reefs (southwestern Atlantic ocean). Cont. Shelf Res. 104175. http://dx.doi.org/10.1016/j.csr.2020.104175.

LI-COR, 2004. LI-7000 CO2/H2O analyzer instruction manual.

Weiss, R.F., Price, B.A., 1980. Nitrous oxide solubility in water and seawater. Mar. Chem. 8, 347–359.

Takahashi, T., Sutherland, S.C., Sweeney, C., Poisson, A., Metzl, N., Tilbrook, B., Bates, N., Wanninkhof, R., Feely, R.A., Sabine, C., et al., 2002. Global sea–air CO 2 flux based on climatological surface ocean pCO 2, and seasonal biological and temperature effects. Deep Sea Res. II 49, 1601–1622.

APHA, 1999. Standard methods for the examination of water and wastewater. p. 2671.

Thermo, S., 2008. User's guide HiPerTOC version: 2.0.3.

Dittmar, T., Koch, B., Hertkorn, N., Kattner, G., 2008. A simple and efficient method for the solid-phase extraction of dissolved organic matter (SPE-DOM) from seawater. Limnol. Oceanogr.: Methods 6, 230–235.

Valderrama, J.C., 1981. The simultaneous analysis of total nitrogen and total phosphorus in natural waters. Mar. Chem. 10, 109–122.

Jeffrey, S.W.t., Humphrey, G.F., 1975. New spectrophotometric equations for determining chlorophylls a, b, c 1 and c 2 in higher plants, algae and natural phytoplankton. Biochem. Physiol. Pflanz. 167, 191–194.

Lamparelli, M.C., 2004. Graus de trofia em corpos d'água do estado de são Paulo: avaliação dos métodos de monitoramento. http://dx.doi.org/10.11606/T.41.2004.tde-20032006-075813.

Lewis, E., Wallace, D., 1998. Program developed for CO2 system calculations ORNL/CDIAC-105. Carbon Dioxide Inf. Anal. Cent. http://dx.doi.org/10.2172/639712.

Dickson, A.G., Millero, F.J., 1987. A comparison of the equilibrium constants for the dissociation of carbonic acid in seawater media. Deep Sea Res. A 34, 1733–1743. http://dx.doi.org/10.1016/0198-0149(87)90021-5.

Lee, K., Kim, T.-W., Byrne, R.H., Millero, F.J., Feely, R.A., Liu, Y.-M., 2010. The universal ratio of boron to chlorinity for the north Pacific and north Atlantic oceans. Geochim. Cosmochim. Acta 74, 1801–1811. http://dx.doi.org/10.1016/J.GCA.2009.12.027.

Weiss, R., 1974. Carbon dioxide in water and seawater: the solubility of a non-ideal gas. Mar. Chem. 2, 203–215.

Raymond, P.A., Cole, J.J., 2001. Gas exchange in rivers and estuaries: Choosing a gas transfer velocity. Estuar. Coasts 24, 312–317.

Borges, A.V., Vanderborght, J.-P., Schiettecatte, L.-S., Gazeau, F., Ferrón-Smith, S., Delille, B., Frankignoulle, M., 2004. Variability of the gas transfer velocity of CO2 in a Macrotidal Estuary (The Scheldt). Estuaries http://dx.doi.org/10.2307/1353473.

Wanninkhof, R., 2014. Relationship between wind speed and gas exchange over the ocean revisited. Limnol. Oceanogr.: Methods 12, 351–362. http://dx.doi.org/10.4319/lom.2014.12.351.

Benson, B.B., Krause, D., 1984. The concentration and isotopic fractionation of oxygen dissolved in freshwater and seawater in equilibrium with the atmosphere' 29. pp. 620–632.

Abril, G., Etcheber, H., Borges, A.V., Frankignoulle, M., 2000. Excess atmospheric carbon dioxide transported by rivers into the scheldt estuary. Comptes Rendus L'Academie Sci.-Ser. IIA-Earth Planet. Sci. 330, 761–768.

Jiang, L.-Q., Cai, W.-J., Wang, Y., 2008. A comparative study of carbon dioxide degassing in river-and marine-dominated estuaries. Limnol. Oceanogr. 53, 2603–2615.

Dias, F.J. da S., Castro, B.M., Lacerda, L.D., Miranda, L.B., Marins, R.V., 2016. Physical characteristics and discharges of suspended particulate matter at the continent-ocean interface in an estuary located in a semiarid region in northeastern Brazil. Estuar. Coast. Shelf Sci. 180, 258–274. http://dx.doi.org/10.1016/j.ecss.2016.08.006.

dos Santos, V.H.M., da Silva Dias, F.J., Torres, A.R., Soares, R.A., Terto, L.C., de Castro, A.C.L., Santos, R.L., Cutrim, M.V.J., 2020. Hydrodynamics and suspended particulate matter retention in macrotidal estuaries located in Amazonia-semiarid interface (northeastern-Brazil). Int. J. Sediment Res. 35, 417–429. http://dx.doi.org/10.1016/j.ijsrc.2020.03.004.

Lima, H.P., Dias, F.J.S., Teixeira, C.E.P., Godoi, V.A., Torres, A.R., Araújo, R.S., 2021. Implications of turbulence in a macrotidal estuary in northeastern Brazil — The são marcos estuarine complex. Reg. Stud. Mar. Sci. 47, 101947. http://dx.doi.org/10.1016/j.rsma.2021.101947.

da Silva Dias, F.J., Lacerda, L.D., Marins, R.V., de Paula, F.C.F., 2011. Comparative analysis of rating curve and ADP estimates of instantaneous water discharge through estuaries in two contrasting Brazilian rivers. Hydrol. Process. 25, 2188–2201. http://dx.doi.org/10.1002/hyp.7972.

Rosentreter, Judith A., Maher, D.T., Erler, D.V., Murray, R., Eyre, B.D., 2018. Factors controlling seasonal CO2 and CH4 emissions in three tropical mangrove-dominated estuaries in Australia. Estuar. Coast. Shelf Sci. 215, 69–82. http://dx.doi.org/10.1016/j.ecss.2018.10.003.

Borges, A.V., Schiettecatte, L.S., Abril, G., Delille, B., Gazeau, F., 2006. Carbon dioxide in European coastal waters. Estuar. Coast. Shelf Sci. 70 (3), 375–387. http://dx.doi.org/10.1016/j.ecss.2006.05.046.

Borges, A.V., Djenidi, S., Lacroix, G., Théate, J., Delille, B., Frankignoulle, M., 2003. Atmospheric CO2 flux from mangrove surrounding waters. Geophys. Res. Lett. 30.

Abril, G., Libardoni, B.G., Brandini, N., Cotovicz, L.C., Medeiros, P.R.P., Cavalcante, G.H., Knoppers, B.A., 2021. Thermodynamic uptake of atmospheric CO2 in the oligotrophic and semi-arid são francisco estuary (NE Brazil). Mar. Chem. 103983. http://dx.doi.org/10.1016/j.marchem.2021.103983.

Cotovicz, L.C., Vidal, L.O., de Rezende, C.E., Bernardes, M.C., Knoppers, B.A., Sobrinho, R.L., Cardoso, R.P., Muniz, M., dos Anjos, R.M., Biehler, A., Abril, G., 2020b. Sources and sinks of CO2 in the delta of the Paraíba do Sul River (southeastern Brazil) modulated by carbonate thermodynamics, gas exchange and ecosystem metabolism during estuarine mixing. Mar. Chem. 226, 103869. http://dx.doi.org/10.1016/j.marchem.2020.103869.

Mounier, S.J.L., Marins, R.V., de Lacerda, L.D., 2018. Determining the influence of urbanization on mangrove zones of northeastern Brazil: Characterization of ceará State Coastal zone organic matter inputs. In: Makowski, C., Finkl, C.W. (Eds.), Threats To Mangrove Forests: Hazards, Vulnerability, and Management, Coastal Research Library. Springer International Publishing, Cham, pp. 199–222. http://dx.doi.org/10.1007/978-3-319-73016-5_10.

Cavalcante, M.S., Marins, R.V., Dias, F.J. da S., Rezende, C.E. de, 2021. Assessment of carbon fluxes to coastal area during persistent drought conditions. Reg. Stud. Mar. Sci. 47, 101934. http://dx.doi.org/10.1016/J.RSMA.2021.101934.

Fry, B., Sherr, E.B., 1989. dl3C measurements as indicators of carbon flow in marine and freshwater ecosystems. In: Stable Isotopes in Ecological Research, Ecological Studies. Springer New York, New York, NY, http://dx.doi.org/10.1007/978-1-4612-3498-2.

de Assis Esteves, F., 1998. Fundamentos de limnologia. Interciência.

Zhai, W., Dai, M., Cai, W.-J., Wang, Y., Wang, Z., 2005. High partial pressure of CO 2 and its maintaining mechanism in a subtropical estuary: the Pearl river estuary, China. Mar. Chem. 93, 21–32.

Marins, R.V., Lacerda, L.D., Araújo, I.C.S., Fonseca, L.V., Silva, F.A.T.F., 2020. Phosphorus and suspended matter retention in mangroves affected by shrimp farm effluents in NE Brazil. An. Acad. Bras. Cienc. 92, 1–15. http://dx.doi.org/10.1590/0001-3765202020200758.

Sánchez-Carrillo, S., Sánchez-Andrés, R., Alatorre, L.C., Angeler, D.G., Álvarez-Cobelas, M., Arreola-Lizárraga, J.A., 2009. Nutrient fluxes in a semi-arid microtidal mangrove wetland in the gulf of California. Estuar. Coast. Shelf Sci. 82, 654–662. http://dx.doi.org/10.1016/J.ECSS.2009.03.002.

Call, M., Ruiz-Halpern, S., Eyre, B.D., Sanders, C.J., Murray, R., Oakes, J.M., Rosentreter, J., Mangion, P., Erler, D.V., Maher, D.T., Santos, I.R., 2014. Spatial and temporal variability of carbon dioxide and methane fluxes over semi-diurnal and spring–neap–spring timescales in a mangrove creek. Geochim. Cosmochim. Acta 150, 211–225. http://dx.doi.org/10.1016/j.gca.2014.11.023.